

# Expression of S100 $\beta$ during mouse cochlear development

Wenjing Liu,<sup>1</sup> Yongchun Zhang,<sup>2</sup> Cheng Liang,<sup>2</sup> Lizhong Su<sup>1</sup>

<sup>1</sup>Otolaryngology & Head and Neck Center, Cancer Center, Department of Otolaryngology, Zhejiang Provincial People's Hospital (Affiliated People's Hospital, Hangzhou Medical College), Hangzhou

<sup>2</sup>Department of Otorhinolaryngology-Head and Neck Surgery, Zhongda Hospital, Southeast University, Nanjing, China

## ABSTRACT

In the present study, the expression of S100 $\beta$  was examined in the mouse cochlea from embryonic day 17 (E17) to postnatal day 32 (P32) using immunofluorescence, aiming to explore its possible role in auditory system. At E17, S100 $\beta$  expression was not detected, except in the external cochlear wall. Starting at E18.5, S100 $\beta$  staining appeared in the organ of Corti and the stria vascularis. In the E18.5 and P1 organ of Corti, S100 $\beta$  was confined to the developing pillar cells. By P6, cytoplasmic staining of S100 $\beta$  was evident in the inner and outer pillar cells, forming the tunnel of Corti. Additionally, S100 $\beta$  expression extended medially into the three rows of Deiter's cells, with labeling of their phalangeal processes. At P8, S100 $\beta$  continued to be expressed in the heads, bodies, and feet of the two pillar cells, as well as in the soma and phalangeal processes of the three rows of Deiter's cells. In the lateral wall of the P8 cochlea, S100 $\beta$  was expressed not only in the stria vascularis but also in the spiral ligament. Between P10 and P12, S100 $\beta$  expression was maintained in the Deiter's cells and pillar cells of the organ of Corti, as well as in the lateral wall, and spiral limbus. From P14 onwards, S100 $\beta$  expression ceased in the stria vascularis, though it persisted in the spiral ligament and spiral limbus into adulthood. Within the P14 and P21 organ of Corti, S100 $\beta$  remained in the Deiter's and pillar cells. S100 $\beta$  immunostaining was not observed in the phalangeal processes of Deiter's cells but was specifically present in the Deiter's cell cups at P21. In the adult cochlea (P28 and P32), S100 $\beta$  expression declined in both Deiter's and pillar cells. The dynamic spatiotemporal changes in S100 $\beta$  expression during cochlear ontogeny suggest its role in cochlear development and hearing function.

**Key words:** S100 $\beta$ ; immunofluorescence; expression; mouse; cochlea; development.

**Correspondence:** Lizhong Su, Otolaryngology & Head and Neck Center, Cancer Center, Department of Otolaryngology, Zhejiang Provincial People's Hospital (Affiliated People's Hospital, Hangzhou Medical College), Hangzhou, China. E-mail: 13588745381@163.com

**Contributions:** WL, study concept and carrying out, manuscript drafting; YZ, CL, LZ, contribution in data analysis and in editing and revising the manuscript. All authors read and approved the final manuscript.

**Conflict of interest:** the authors declared no potential conflicts of interest with respect to the research, authorship, and publication of this article.

**Ethical approval:** all animal studies, including the euthanasia procedure, were conducted in compliance with the regulations and guidelines of Southeast University's institutional animal care, adhering to the standards set by the Association for Assessment and Accreditation of Laboratory Animal Care (AAALAC) and the Institutional Animal Care and Use Committee (IACUC) guidelines (approval No. 20200402025).

**Availability of data and material:** the data used to support the findings of this study are available from the corresponding author upon reasonable request.

**Funding:** this work was supported by the National Natural Science Foundation of China (No. 82000987) and the Natural Science Foundation of Jiangsu Province (No. BK20200394).

## Introduction

Several members of the EF-hand calcium-binding protein family, including calbindin-D28K, calretinin, parvalbumin, and S100 proteins,<sup>1-4</sup> have been widely expressed in the cochlea, providing important clues about their roles in cochlear organogenesis and function. Recently, the importance of S100 proteins in hearing was highlighted, with changes in their expression in the mouse cochlea implicated in congenital hearing loss in Waardenburg syndrome due to Pax3 loss.<sup>5</sup> Among the EF-hand calcium-binding protein, the low-molecular-weight S100 proteins, which consist of twenty members, represent the largest subgroup.<sup>6</sup> S100 proteins form dimers, primarily consisting of S100a and S100 $\beta$  subunits.<sup>7</sup> In comparison to the numerous members of the S100a subfamily, the S100 $\beta$  subfamily mainly includes S100 $\beta$ . S100 $\beta$ , a soluble calcium-binding protein of 21 kDa, is the most active member of the S100 protein family and the most abundant in the central nerve system,<sup>8,9</sup> where it is primarily released by glial cells.<sup>10</sup> Deregulated expression of S100 $\beta$  has been implicated in neurodegeneration, inflammation, and brain damage.<sup>11-13</sup> Additionally, S100 $\beta$  has been used as a diagnostic and prognostic marker in clinical settings based on its concentration in serum or cerebrospinal fluid.<sup>14,15</sup> However, the exact physiological functions of S100 proteins in the cochlea and normal hearing remain unclear. Age-dependent expression of S100 $\beta$  has been reported in the brains of mice.<sup>16</sup> Previous immunohistochemical studies have demonstrated the distribution of S100 immunostaining in the cochleas of several species, including guinea pigs, mice, rats, and humans, though some inconsistencies in the findings exist. For example, in rats, S100 immunolabeling was reported in the inner sulcus cells and inner phalangeal cells.<sup>17</sup> While S100 is widely expressed in the supporting cells of the mouse and guinea pig organ of Corti,<sup>18,19</sup> it has not been reported as a key marker protein in spiral ligament fibrocytes.<sup>20</sup> In the human embryonic cochlea, S100 expression was restricted to the spiral ligament, Reissner's membrane, and spiral limbus.<sup>21</sup> Strain differences and variations in staining techniques may explain this variability. Although S100a and S100 $\beta$  share a high degree of sequence and structural similarity, their differential localization in various tissues indicates functional discrepancies.<sup>22</sup> To date, only one study has reported the spatiotemporal expression of S100a in the cochlea during postnatal development.<sup>23</sup> However, the cellular distribution of S100 $\beta$  in both the adult and developing cochlea remains limited. Therefore, our present study aimed to examine the dynamic expression patterns of S100 $\beta$  across various developmental stages. We report that S100 $\beta$  is preferentially distributed in the supporting cells of the organ of Corti and the lateral wall of the mouse cochlea, with its expression developmentally regulated, closely following cochlear maturation.

## Materials and Methods

### Animals

All animal studies, including the euthanasia procedure, were conducted in compliance with the regulations and guidelines of Southeast University's institutional animal care, adhering to the standards set by the Association for Assessment and Accreditation of Laboratory Animal Care (AAALAC) and the Institutional Animal Care and Use Committee (IACUC) guidelines (approval No. 20200402025).

## Immunofluorescence

Pregnant BALB/c mice (gestational days 17-18.5) and postnatal mice (P1-P32) were anesthetized by intraperitoneal injection of 10% chloral hydrate (0.2 mL/100 g). Postnatal mice were intracardially perfused with saline followed by 4% paraformaldehyde in 0.1 M phosphate buffer (pH 7.4). Detailed methods for immunofluorescent staining were described in our previous study.<sup>24,25</sup> Briefly, after perilymphatic perfusion with the fixative, the cochlea was postfixed in the same solution for 35 min at room temperature. Cochlea from mice older than P5 were decalcified in 10% EDTA (pH 7.4). Following decalcification, the cochleas were immersed in a sucrose gradient (15% for 3 h and 30% overnight). Cochlear tissues were then embedded in optimum cutting temperature compound at 4°C for 2.5 h, rapidly frozen at -20°C, and cryoembedded specimens were sectioned into serial sections (8  $\mu$ m) using a cryostat and mounted on glass slides.

Cochlear cryosections were treated with 10% donkey serum and 0.3% Triton X-100 in PBS for 45 min at room temperature to enhance cell membrane permeability to antibodies. The sections were then incubated with primary antibodies, diluted in 0.01M PBS overnight or longer at 4°C. The primary antibodies used were as follows: rabbit anti-S100 $\beta$  antibodies (1:500, #90393; Cell Signaling Technology, Danvers, MA, USA), Sox2 Monoclonal Antibody (Btjce; Invitrogen, Waltham, MA, USA), Alexa Fluor™ 488 (1:100, #53-9811-82; Invitrogen), biotinylated isolectin B4 antibody (1:250, Vector Laboratories, Newark, CA, USA). In double-stained experiments, coralite594-conjugated phalloidin (1:250, #PF00003; Proteintech, Wuhan, China) was applied to detect F-actin in the hair cells of the organ of Corti. After rinsing three times for 15 min in 0.01 M PBS, the slides were incubated for 1 h at 37°C with the following secondary antibodies: donkey anti-rabbit IgG conjugated with Alexa fluor 488 or 555 (1:250; Yeasen Biotechnology, Shanghai, China), Streptavidin conjugated with Alexa fluor 594 (1:250; Yeasen Biotechnology). Control sections were incubated with 0.01 M PBS, without primary antibodies. Additionally, rabbit (DA1E) monoclonal antibody IgG XP Isotype control (#3900; Cell Signaling Technology) was used as a negative control, in place of the S100 $\beta$  antibody. The sections were then washed with PBS, and fluorescence was preserved by sealing the specimens with an antifade mounting medium containing 4',6-diamidino-2-phenylindole (Biyuntian, Biotechnology, Shanghai, China). Cryostat sections were examined using a Zeiss (LSM900) laser scanning confocal microscope with 10 $\times$  (NA= 0.45), 20 $\times$  (NA = 0.8), 40 $\times$  (NA = 0.95) and 63 $\times$  oil (NA = 1.4) objectives at 1024  $\times$  1024 pixels. Zen3.0 acquisition software was used. Immunostaining presented in figures is representative of three individual experiments. Images were cropped and resized using Adobe Photoshop CC 2019.

## Results

### Expression patterns of S100 $\beta$ in the mouse cochlea during the late embryonic stages of development by immunofluorescence

The expression patterns of S100 $\beta$  were analyzed in the mouse cochlea from E17 to adulthood using immunofluorescence staining and confocal microscopy. At E17 (the earliest age examined), double-labeling with S100 $\beta$  and the supporting cell marker Sox2, which labeled parts of the greater epithelial ridge, inner hair cells (IHCs), three rows of outer hair cells (OHCs), and Deiters' cells located above the basement membrane during the late embryonic stages,<sup>26</sup> showed no immunoreactivity for S100 $\beta$  in the Sox2-

marked auditory epithelium. S100 $\beta$  immunoreactivity was observed only in the external cochlear wall (Figure 1 A-C). Beginning at E18.5, similar to previously reported S100 expression patterns,<sup>5</sup> S100 $\beta$  staining first appeared in the auditory epithelium. S100 $\beta$  expression occurred in both the apical and basal regions of the developing pillar cells. S100 $\beta$ -immunolabeled pillar cells separated Sox2-marked IHCs from OHCs. Expression of

S100 $\beta$  was also present in the marginal and intermediate cells of the stria vascularis (Figure 1 D-I). No immunofluorescence labeling of S100 $\beta$  was detected in any parts of the E18.5 cochlea in negative controls omitting the primary antibody. Also, no antibody binding was observed in negative controls stained with normal rabbit IgG (*Supplementary Figure S1*).

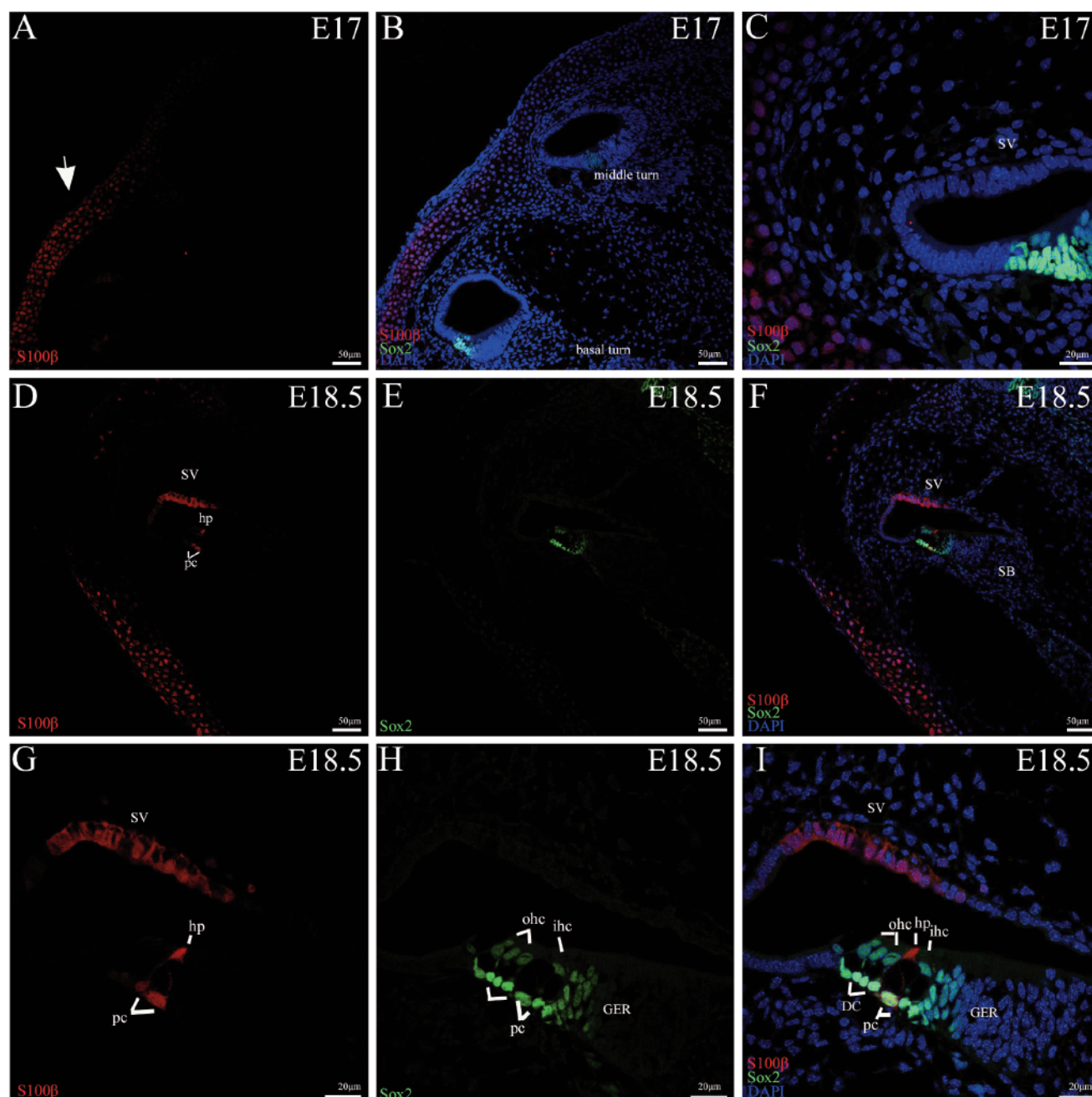


**Figure 1.** S100 $\beta$  immunolabeling in the mouse cochlea at E17 and E18.5. **A-C)** In the mouse cochlea at E17, S100 $\beta$  immunoreactivity was only observed in the external cochlear wall (arrowheads), with no labeling detected in other cochlear tissues. Double-labeling with S100 $\beta$  and Sox2 revealed that no S100 $\beta$  immunoreactivity was present in the Sox2-immunoreactive auditory epithelium. **D-I)** In the middle turn of the mouse cochlea at E18.5, S100 $\beta$  immunoreactivity was predominantly detected in the apical region of the developing pillar cells. S100 $\beta$ -labeled pillar cells were located between the Sox2-labeled IHCs and the first row of OHCs. The base of the pillar cells was also labeled with S100 $\beta$ . Additionally, the stria vascularis showed immunoreactivity for S-100 $\beta$ . IHC, inner hair cell; OHC, outer hair cell; SV, stria vascularis; GER, greater epithelial ridge; pc, pillar cells; DC, Deiters' cells; hp, head plate; SB, the spiral limbus.



## Expression patterns of S100 $\beta$ in the mouse cochlea during postnatal development by immunofluorescence

In P1 mice, S100 $\beta$  immunostaining was maintained in the stria vascularis in the apical and middle turns, while no S100 $\beta$  labeling was observed in the Sox2-marked auditory epithelium in the apical

turn (Figure 2 A,B). Phalloidin, a marker for F-actin, labeled the surface of the greater epithelial ridge and the cuticular plates of the IHCs and OHCs at this stage.<sup>27</sup> Co-staining of S100 $\beta$  with phalloidin and Sox2 demonstrated that S100 $\beta$ -immunoreactive inner and outer pillar cells were interposed between the IHCs and OHCs. S100 $\beta$  was clearly expressed in the developing inner and outer pillar cells, particularly in the foot plates of the pillar cells sitting atop

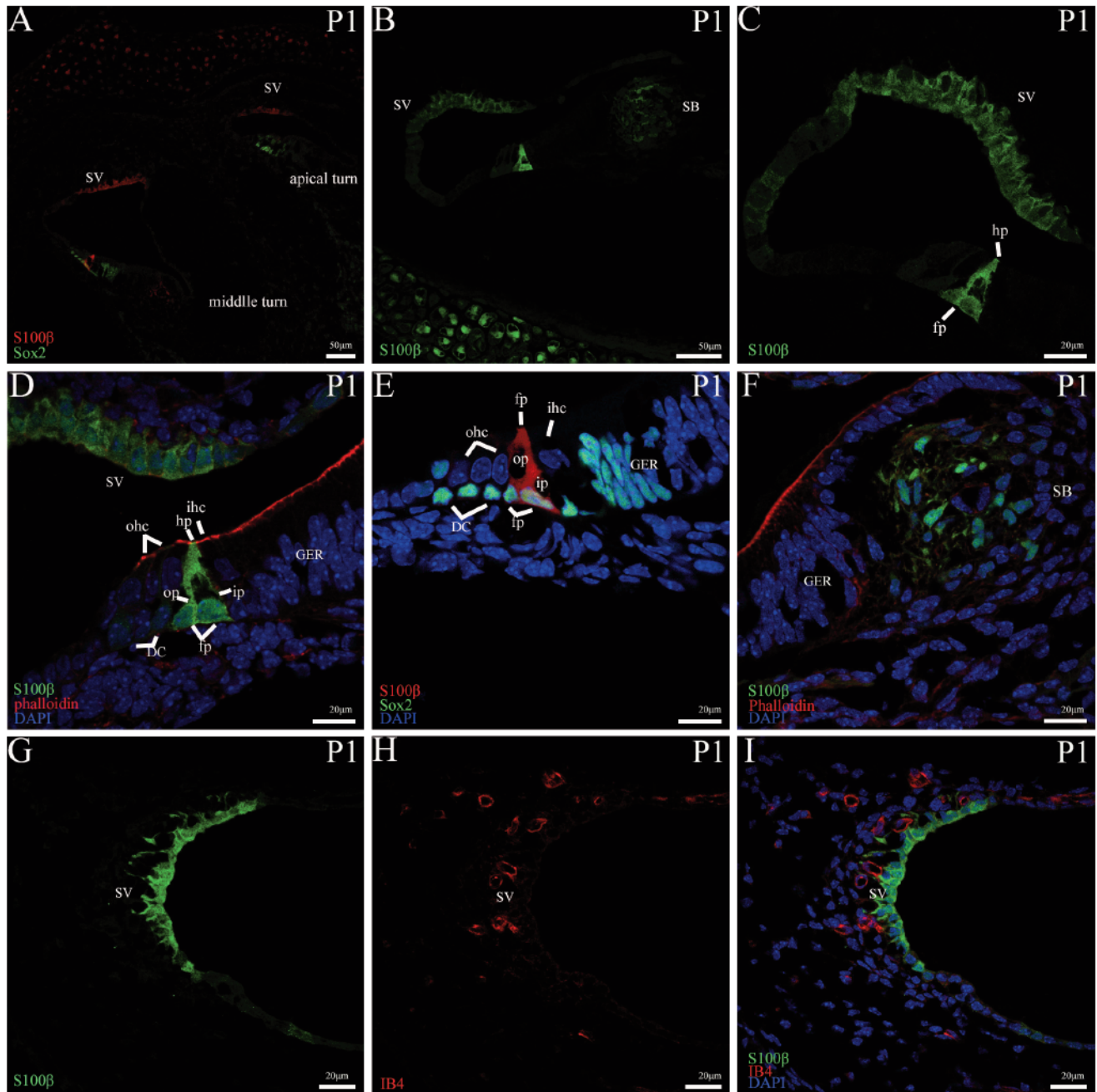


**Figure 2.** S100 $\beta$  immunolabeling in the mouse cochlea at P1. **A)** A low-magnification view of cross-sections of the P1 mouse cochlea labeled with S100 $\beta$  (red) and Sox2 (green) at P1. S100 $\beta$  immunoreactivity was not detected in the organ of Corti in the apical turn at P1. **B,C)** In the middle turn of the P1 cochlea, the stria vascularis and pillar cells of the organ of Corti were S100 $\beta$ -labeled. **D,E)** Co-staining S100 $\beta$  with phalloidin (red) and Sox2 (green) revealed that S100 $\beta$ -labeled inner and outer pillar cells were positioned at the boundary between the phalloidin-marked IHCs and OHCs. S100 $\beta$ -positive cells were predominantly observed in the head and foot plates of the pillar cells. **F)** S100 $\beta$  expression was also detected in the spiral limbus. **G-I)** Double-labeling with S100 $\beta$  (green) and IB4 (red) demonstrated that S100 $\beta$ -positive cells in the stria vascularis were in close proximity to IB4-marked intrastrial capillaries. IHC, inner hair cell; OHC, outer hair cell; SV, stria vascularis; GER, greater epithelial ridge; ip, inner pillar cells; op, outer pillar cells; DC, Deiters' cells; hp, head plate; fp, footplate; SB, the spiral limbus.



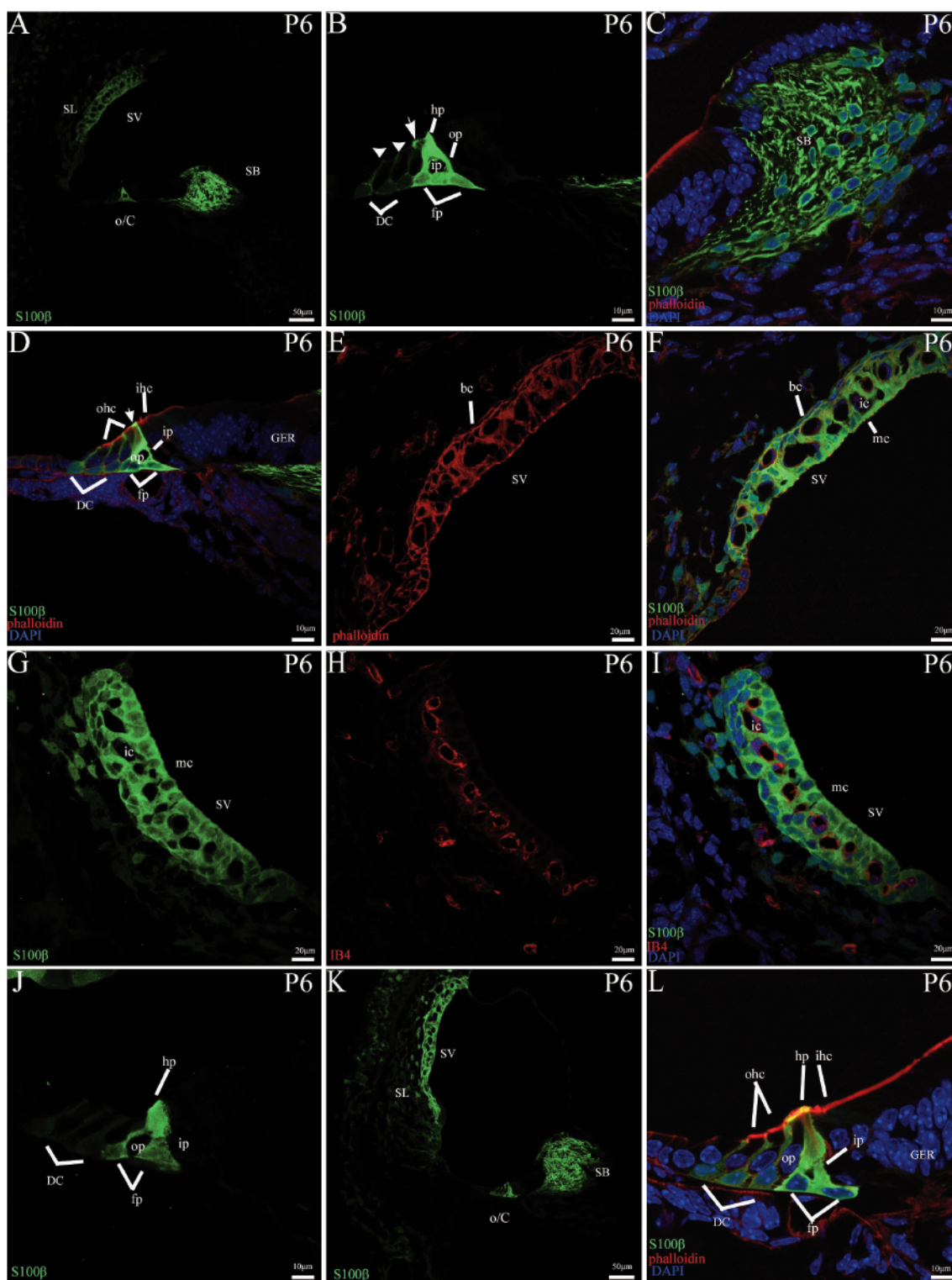


**Figure 3.** S100 $\beta$  immunolabeling in the mouse cochlea at P6. **A-B)** At the middle turn of the P6 cochlea, S100 $\beta$  staining was present throughout the cell bodies of both inner and outer pillar cells, which were separated to form the tunnels of Corti. The apices of the S100 $\beta$ -expressing pillar cells projected laterally (arrowhead) to contact the OHCs. Labelling for S100 $\beta$  was observed in the three rows of Deiters' cells, with S100 $\beta$ -expressing Deiters' cells positioned at the base of each OHC, extending a long phalangeal process (arrows) between the base and the apex of the OHCs. **C)** S100 $\beta$  labeling was also seen in the spiral limbus. **D)** Double-labeling of S100 $\beta$  with phalloidin showed that S100 $\beta$ -labeled Deiters' cell phalangeal processes extending between rows of OHCs. **E,F)** S100 $\beta$  expression was localized to stria marginal cells facing the scale media, S100 $\beta$  colocalized with phalloidin in the basal cells of the stria vascularis. **G-I)** stria intermediate cells that located around the IB4-labeled stria capillaries were immunopositive for S100 $\beta$ . **J-L)** In both the apical and basal turns of the P6 cochlea, S100 $\beta$  was also expressed in the outer and inner pillar cells and the three rows of Deiters' cells. IHC, inner hair cell; OHC, outer hair cell; SV, stria vascularis; GER, greater epithelial ridge; ip, inner pillar cells; op, outer pillar cells; DC, Deiters' cells; hp, head plate; fp, footplate; SB, the spiral limbus; mc, the marginal cells; ic, the intermediate cells; bc, the basal cells; o/C, organ of Corti.

the basilar membrane, whereas it remained unexpressed in Deiters' cells (Figure 2 C-E). Additionally, S100 $\beta$  began to be detected in the spiral limbus (Figure 2F). S100 $\beta$  showed a cytoplasmic distribution in the stria vascularis, capillaries of the stria vascularis

labeled by isolectin B4 (IB4), a specific vascular endothelial marker, were not positive for S100 $\beta$  (Figure 2 G-I).<sup>28</sup> At P6, the bodies of the labeled inner and outer pillar cells moved apart, forming the future triangular, fluid-filled space known as the tunnel of Corti.<sup>29</sup>

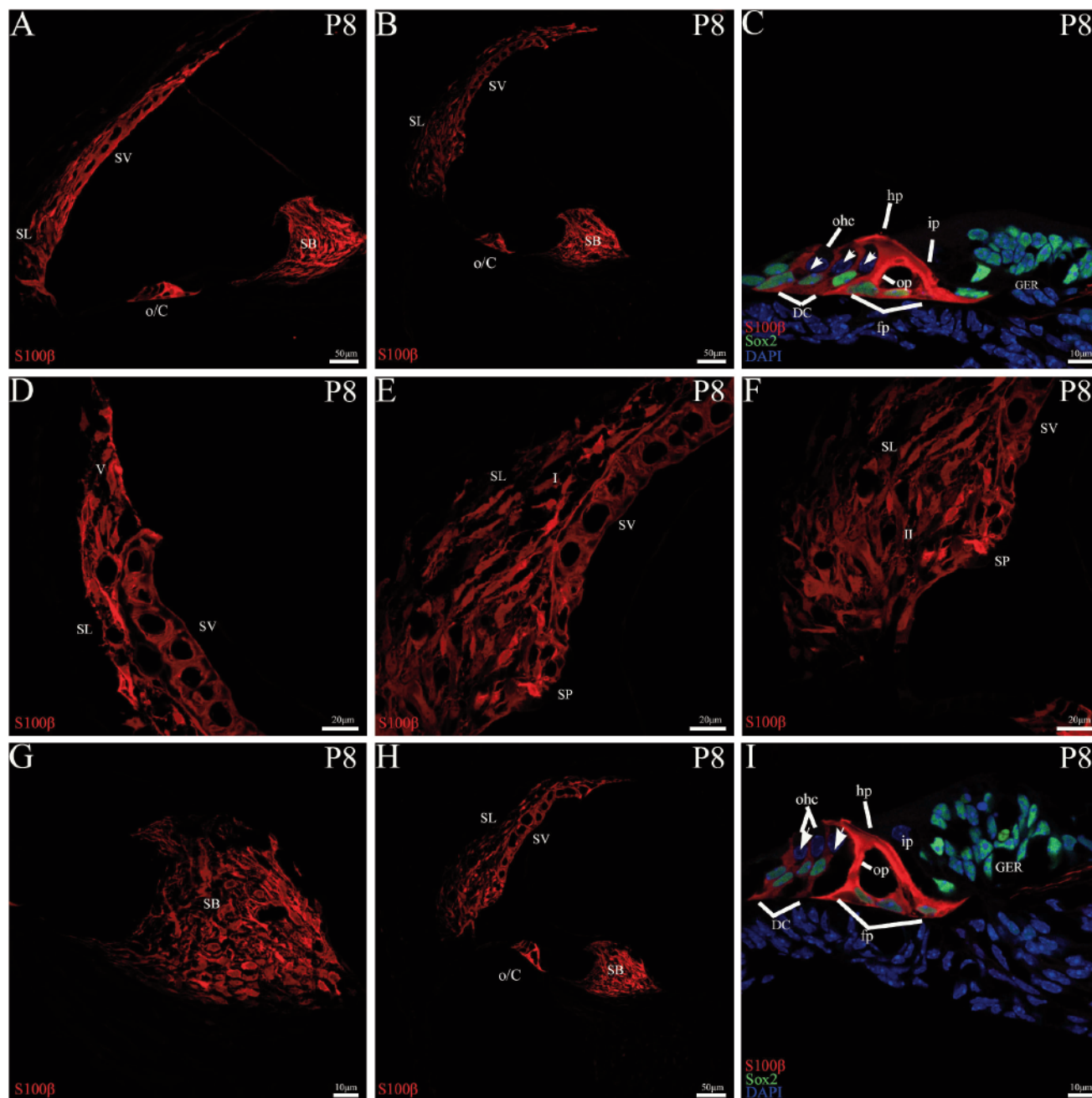


**Figure 4.** S100 $\beta$  immunolabeling in the mouse cochlea at P8. **A,B**) At P8, S100 $\beta$  staining was observed in the organ of Corti, spiral ligament, stria vascularis, and spiral limbus in the apical and medial turns. **C**) Double-labeling with S100 $\beta$  and Sox2 showed that S100 $\beta$  staining was uniformly distributed throughout the cytoplasm of the pillar cells, from the head plate toward the footplate. The phalangeal processes (arrows) of Deiters' cells developed into finger-like structures. **D-F**) The spiral ligament was largely immunoreactive for S100 $\beta$ , including type I fibrocytes lateral to the stria vascularis, type II fibrocytes under the spiral prominence, and type V fibrocytes above the Resissner's membrane lining the scala vestibuli. **G**) Fibrocytes in the spiral limbus were expressed by S100 $\beta$ . **H,I**) In the P8 basal turns, S100 $\beta$  immunoreactivity occurred in the Deiters' cell cup region (arrows) which enveloped the base of the outer hair cell. IHC, inner hair cell; OHC, outer hair cell; SV, stria vascularis; GER, greater epithelial ridge; ip, inner pillar cells; op, outer pillar cells; DC, Deiters' cells; hp, head plate; fp, footplate; SB, the spiral limbus; o/C, organ of Corti; SP, the spiral prominence; Roman numerals indicate fibrocyte types.

S100 $\beta$  expression was observed throughout the cell bodies of pillar cells, and noteworthy, S100 $\beta$  immunostaining was also present in the transcellular processes of the pillar cells and spiral limbus (Figure 3 A-C). S100 $\beta$ -labeled Deiters' cells were easily distinguished by their phalangeal processes lying below the cuticular plates of OHCs, labeled with phalloidin (Figure 3D). We also found that the stria vascularis, including marginal, intermediate,

and basal cells, expressed S100 $\beta$ . Cytoplasmic S100 $\beta$  labeling was detected in the three cellular layers of the stria vascularis. Co-staining of S100 $\beta$  with phalloidin, a marker for the basal cells of the stria vascularis, revealed co-expression in the basal cells (Figure 3 E,F).<sup>30</sup> Intermediate cells present in close vicinity with IB4-labelled intrastrial capillaries were also immunostained for S100 $\beta$  (Figure 3 G-I). No obvious apical-basal gradient for S100 $\beta$

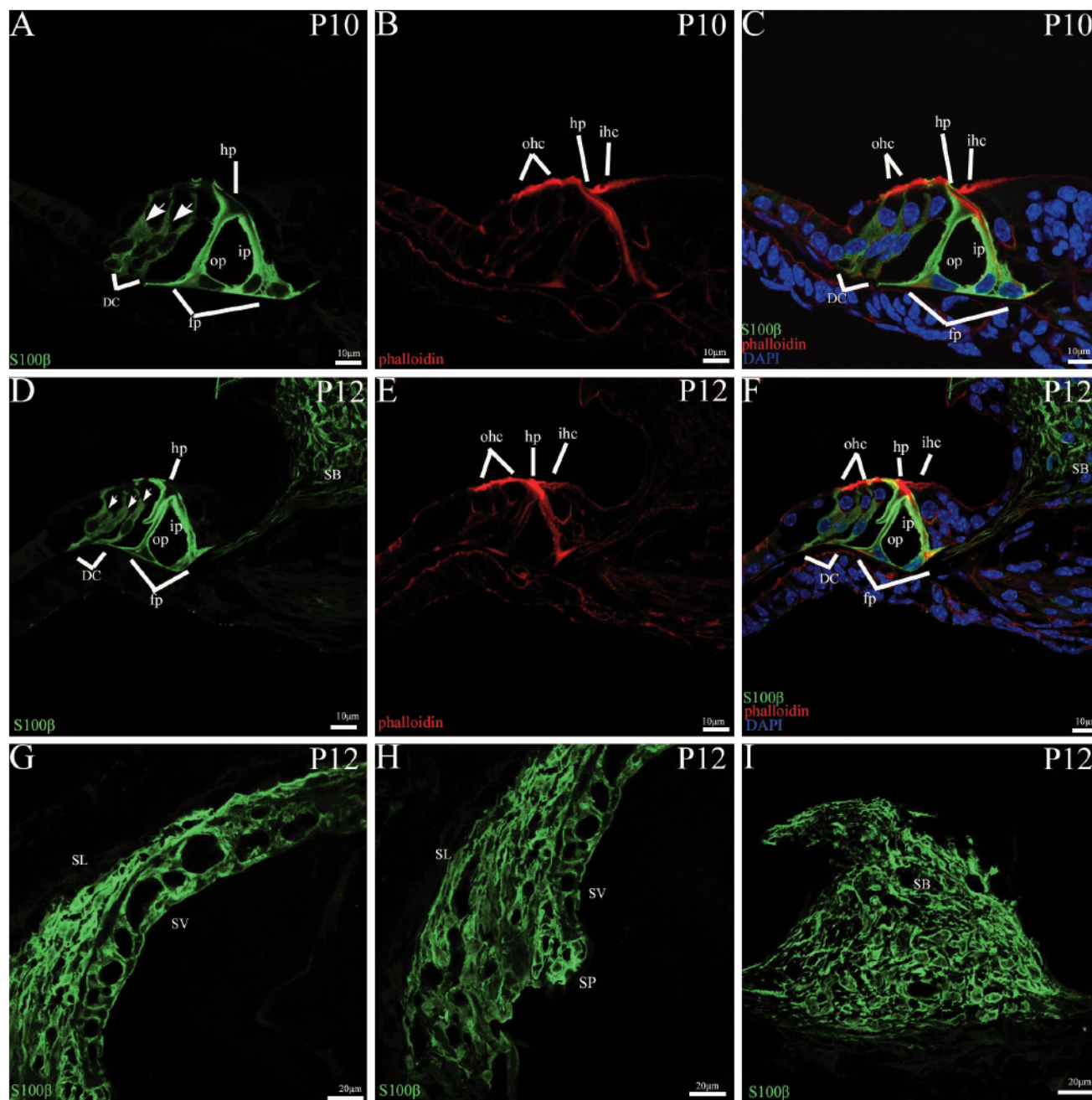


**Figure 5.** S100 $\beta$  immunolabeling in the mouse cochlea at P10 and P12. **A-C**) At P10, double staining of S100 $\beta$  and phalloidin revealed that S100 $\beta$ -labeled Deiters' cell phalangeal processes were clearly located below the phalloidin-stained cuticular plate of OHCs. S100 $\beta$  expression was also observed in the Deiters' cups (arrowheads), which held the OHCs at their base. Notably, the center of the head region of pillar cells, rich in phalloidin-marked actin, was unlabeled for S100 $\beta$ . **D-I**) At P12, S100 $\beta$ -expressing cells were observed in the inner and outer pillar cells, the soma and phalangeal processes of the Deiters' cells, the spiral limbus, the stria vascularis, and the spiral ligament. The Deiters' cups (arrowheads) were also immunoreactive for S100 $\beta$ . IHC, inner hair cell; OHC, outer hair cell; SV, stria vascularis; SL, the spiral ligament; GER, greater epithelial ridge; ip, inner pillar cells; op, outer pillar cells; DC, Deiters' cells; hp, head plate; fp, footplate; SB, the spiral limbus; SP, the spiral prominence.



immunoreactivity was observed in the P6 organ of Corti (Figure 3 J-L). By P8, S100 $\beta$  expression was seen in the spiral ligament fibrocytes, and its expression in the spiral ligament was consistent with it being a marker for type I, II, and V fibroblasts. S100 $\beta$  showed a similar pattern in the organ of Corti across the apical, middle, and basal turns. S100 $\beta$  continued to be homogeneously expressed in the inner and outer pillar cells. S100 $\beta$ -labeled the head of inner pillar cells extending over the top of the outer pillar

cells and projecting laterally to contact the first row of OHCs. S100 $\beta$ -labeled Deiters' cells also showed cytoplasmic S100 $\beta$  expression, with the phalangeal processes projecting from the bases to the apex of the OHCs. In the spiral limbus, S100 $\beta$  labeling was mainly found in the limbal fibrocytes beneath the interdental cells (Figure 4 A-I). By P10, approximately at the onset of hearing, S100 $\beta$ -positive inner and outer pillar cells further elongated. The nuclei of the footplates of the two pillar cells moved apart, forming

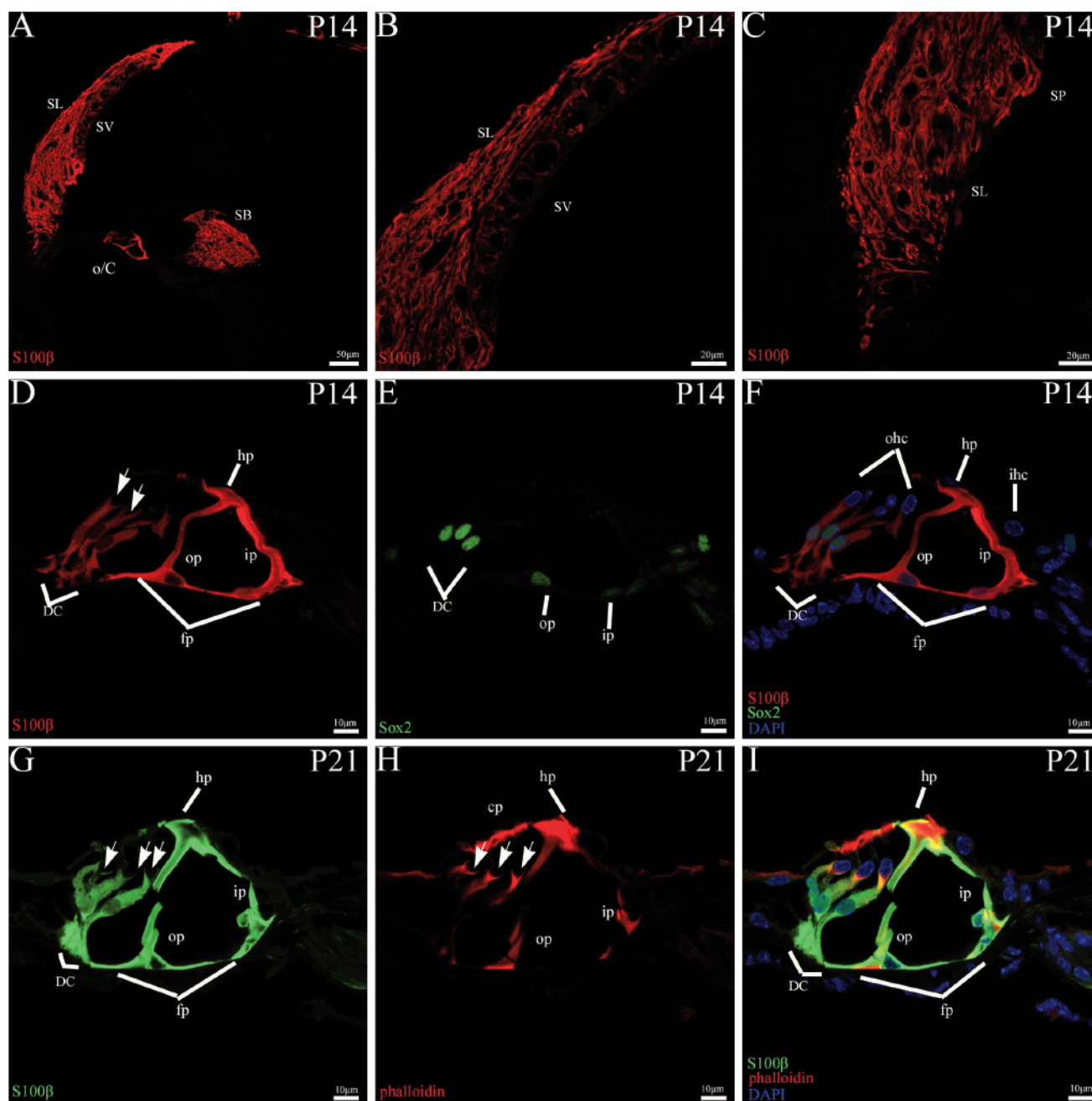


**Figure 6.** S100 $\beta$  immunolabeling in the mouse cochlea at P14 and P21. **A-C)** At P14, S100 $\beta$  expression in the stria vascularis disappeared but was maintained in the spiral ligament. **D-F)** S100 $\beta$  staining in the phalangeal processes of Deiters' cells was ambiguous, although the bodies and cups (arrowheads) of the Deiters' cells remained immunoreactive. **G-I)** At P21, phalloidin-marked actin labeling was prominent in the pillar cell foot and head, as well as in the Deiters' cups. Overlapping labeling of S100 $\beta$  and phalloidin was observed in Deiters' cups and the apex of pillar cells. IHC, inner hair cell; OHC, outer hair cell; SV, stria vascularis; SL, the spiral ligament; GER, greater epithelial ridge; ip, inner pillar cells; op, outer pillar cells; DC, Deiters' cells; hp, head plate; fp, footplate; SB, the spiral limbus; o/C, organ of Corti.

the typical triangular structure of the tunnel of Corti. Additionally, S100 $\beta$  was expressed not only in the phalangeal processes and bodies of Deiters' cells, but also in the Deiters' cell cups, which envelop the base of the OHCs (Figure 5 A-C).<sup>31</sup> At the onset of hearing (P12), S100 $\beta$  expression in the cochlea was similar to that observed at P10. S100 $\beta$  continued to be expressed in the Deiters' cells, pillar cells, spiral limbus, and cochlear lateral wall (Figure 5

G-I). After the onset of hearing, as Deiters cell processes became thinner,<sup>32</sup> S100 $\beta$  staining in the phalangeal processes of Deiters' cells became ambiguous. From P14 onwards, the stria vascularis no longer expressed S100 $\beta$  (Figure 6 A-F). By P21, S100 $\beta$  remained expressed in the somata and cups of Deiters' cells, as well as in the head, bodies, and feet of pillar cells (Figure 6 G-I). The expression of S100 $\beta$  was also maintained in the fibrocytes of

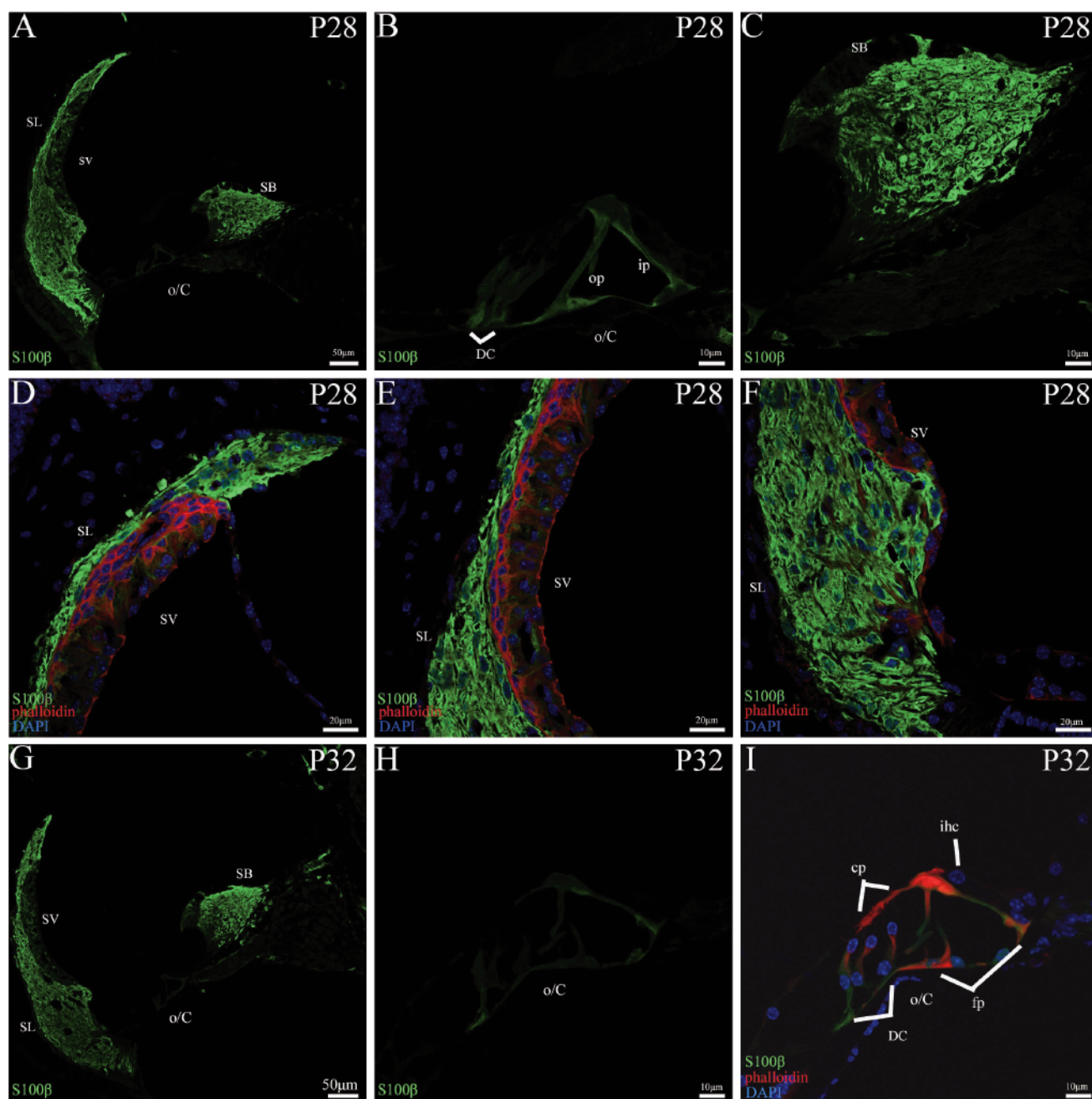


**Figure 7.** S100 $\beta$  immunolabeling in the mouse cochlea at P28 and P32. **A,B)** At P28, S100 $\beta$  expression declined in both the pillar cells and the Deiters' cells. **C)** The spiral limbus was still positive for S100 $\beta$ . **D-F)** No S100 $\beta$  staining was observed in the phalloidin-marked basal cells of the stria vascularis. S100 $\beta$  immunolabeling was seen throughout the spiral ligament. **G-I)** At P32, S100 $\beta$  expression was only detected in the spiral ligament and the spiral limbus, phalloidin-labeled pillar cells and Deiters' cells in the organ of Corti barely expressed S100 $\beta$ . IHC, inner hair cell; OHC, outer hair cell; SV, stria vascularis; SL, the spiral ligament; ip, inner pillar cells; op, outer pillar cells; DC, Deiters' cells; hp, head plate; fp, footplate; SB, the spiral limbus; o/C, organ of Corti.

the late postnatal and adult spiral ligament and spiral limbus. However, but by adult ages (P28 and P30), S100 $\beta$  expression was selectively downregulated in the Deiters' cells and pillar cells in the organ of Corti (Figure 7 A-I).

## Discussion

In this study, we present the first comprehensive description of the expression of S100 $\beta$  in the developing and mature mouse cochlea. Dynamic changes in S100 $\beta$  expression were observed during cochlear maturation, suggesting its involvement in cochlear development. S100 $\beta$ , a cytoplasmic calcium-binding protein primarily expressed by glia, acts as a neurotrophic factor that promotes neurite maturation and outgrowth during the development of the nervous system.<sup>33,34</sup> Supporting cells of the organ of Corti share important similarities with glial cells and may perform functions comparable to those of glial cells or astrocytes in the central nervous system and retina.<sup>35,36</sup> Vimentin and glial fibrillary acidic protein, two glial-derived marker, are commonly used as marker for supporting cells of the organ of Corti.<sup>37,38</sup> Our results showed that S100 $\beta$  was uniformly distributed throughout the cytoplasm of the pillar cells and Deiters' cells, including the phalangeal processes of all three Deiters' cells, as well as the head, body, and feet of both inner and outer pillar cells. This labeling pattern of S100 $\beta$  supports its role as an excellent marker for supporting cells in the organ of Corti. It has been proposed that key morphological events related to cochlear function occur before P12, including the structural and anatomical remodeling of Deiters' cells and pillar cells.<sup>39,40</sup> Prior to and during the onset of hearing, the feet of the pillar cells separate, leading to the formation and opening of the triangular fluid-filled space known as the tunnel of Corti, which marks a milestone in the maturation of the organ of Corti.<sup>41,42</sup> During this period, Deiters' cells also undergo dramatic changes in cell shape, one of the most striking being the formation of cups in the Deiters' cell bodies.<sup>43</sup> As a docking site for the bottom of the OHCs, the cup of Deiters' cell has been suggested to be associated with wound healing.<sup>44</sup> The results of this study demonstrated that S100 $\beta$  first appeared in the developing pillar cells of the organ of Corti at later embryonic stages, while Deiters' cells began expressing S100 $\beta$  during the early neonatal period. As the support cells further differentiate, S100 $\beta$  expression in the two pillar cells and three Deiters' cells persisted after the onset of hearing, coinciding with the pre-opening and full opening of the tunnel of Corti, as well as the formation of the Deiters' cell cups. Thus, S100 $\beta$  expression may play a role in the differentiation and maturation of supporting cells in the organ of Corti, contributing to cochlear development. Moreover, the phalangeal processes of Deiters' cells and the head of pillar cells, both expressing S100 $\beta$ , constituted part of the reticular lamina. This lamina serves as a barrier separating the endolymph and perilymph, and this fluid barrier is essential for cochlear function.<sup>45</sup> Supporting cells in the cochlea are thought to maintain the homeostasis of the organ of Corti and contribute to the sound transduction of the hair cells.<sup>46,47</sup> In the adult mouse cochlea, our results demonstrated age-related changes in S100 $\beta$  expression, with downregulated expression observed in supporting cells. Changes in the immunoreactivity of calcium-binding proteins have been reported with aging, due to their capacity to buffer Ca<sup>2+</sup> and protect against Ca<sup>2+</sup> overload,<sup>48,49</sup> which becomes more prominent during aging and degeneration. Additionally, abnormal expression of S100 $\beta$  has been proposed to be linked to age-related diseases, including Alzheimer's disease.<sup>50,51</sup> Changes in S100 $\beta$  protein expression in the adult cochlea may conceivably be related to aging and hearing loss.

Besides the organ of Corti, S100 $\beta$  was also shown in this study

to be expressed in the stria vascularis, spiral ligament, and spiral limbus, marking a clear distinction from S100a, which has been reported to be exclusively expressed in the intermediate cells of the stria vascularis after the onset of hearing. This result aligns with the idea that different S100 family members have a cell type-specific distribution in various tissues.<sup>52</sup> The dynamics of S100 $\beta$  expression in the stria vascularis and spiral ligament are particularly noteworthy. The stria vascularis is known to be essential for generating of the endocochlear potential (EP) and secreting potassium into the endolymph.<sup>53,54</sup> EP is the driving force for hair cell mechanotransduction, which plays a crucial role in hearing.<sup>55,56</sup> The developmental processes of EP in the mouse cochlea have been documented, with EP onset occurring around P1 and increasing abruptly from P9 to P16. By P17, EP reaches a mature level.<sup>57,58</sup> Prior to the onset of EP, S100 $\beta$  expression was evident in the stria vascularis and spiral limbus before birth. Before P12, coinciding with the rapid rise in EP, S100 $\beta$  expression was maintained in the stria vascularis. Thus S100 $\beta$  may be involved in the development of EP. Given that it is widely accepted that fibrocytes of the spiral ligament and spiral limbus work together to maintain cochlear ion homeostasis,<sup>59,60</sup> and considering that S100 $\beta$ -marked glia cells function to maintain retinal and brain homeostasis, these results further support the involvement of S100 $\beta$  in regulating this process.<sup>61-63</sup> There is considerable evidence indicating that inflammation is a component of the mechanisms underlying age-related hearing loss,<sup>64,65</sup> much like its critical role in the pathogenesis of aging-related diseases.<sup>66,67</sup> As an important mediator of inflammation,<sup>68</sup> the significance of S100 $\beta$  is underscored by its deregulated expression in neurodegenerative and inflammatory disorders.<sup>69,70</sup> The lateral wall of the cochlea, particularly the spiral ligament, is a frequent site of inflammation,<sup>71</sup> and exhibited selective expression of S100 $\beta$  during adulthood. This finding further supports the hypothesis of its potential involvement in presbycusis, warranting further studies to clarify this possibility.

This paper revealed the developmentally-regulated expression of S100 $\beta$  in the mouse cochlea, where it was specifically expressed in the developing supporting cells of the organ of Corti, the stria vascularis, the spiral limbus, and the spiral ligament. These results suggest that S100 $\beta$  plays an important role in cochlear development and the establishment of hearing functions.

## References

1. Liu W, Chen H, Zhu X, Yu H. Expression of calbindin-D28K in the developing and adult mouse cochlea. *J Histochem Cytochem* 2022;70:583-96.
2. Liu W, Zhang Y, Liang C, Jiang X. Developmental expression of calretinin in the mouse cochlea. *Eur J Histochem* 2024;68:4137.
3. Yang D, Thalmann I, Thalmann R, Simmons DD. Expression of alpha and beta parvalbumin is differentially regulated in the rat organ of Corti during development. *J Neurobiol* 2004;58:479-92.
4. Foster JD, Drescher MJ, Hatfield JS, Drescher DG. Immunohistochemical localization of S-100 protein in auditory and vestibular end organs of the mouse and hamster. *Hear Res* 1994;74:67-76.
5. Udagawa T, Takahashi E, Tatsumi N, Mutai H, Saijo H, Kondo Y, et al. Loss of Pax3 causes reduction of melanocytes in the developing mouse cochlea. *Sci Rep* 2024;14:2210.
6. Rezvanpour A, Phillips JM, Shaw GS. Design of high-affinity S100-target hybrid proteins. *Protein Sci* 2009;18:2528-36.
7. Arrais AC, Melo LHMF, Norrara B, Almeida MAB, Freire KF, Melo AMMF, et al. S100B protein: general characteristics and pathophysiological implications in the central nervous system.



- Int J Neurosci 2022;132:313-21.
8. Yordan T, Erenler AK, Baydin A, Aydin K, Cokluk C. Usefulness of S100B protein in neurological disorders. *J Pak Med Assoc* 2011;61:276-81.
  9. Hernández-Ortega K, Canul-Euan AA, Solis-Paredes JM, Borboa-Olivares H, Reyes-Muñoz E, Estrada-Gutierrez G, Camacho-Arroyo I. S100B actions on glial and neuronal cells in the developing brain: an overview. *Front Neurosci* 2024;18:1425525.
  10. Karlsson O, Berg AL, Lindström AK, Hanrieder J, Arnerup G, Roman E, et al. Andersson M. Neonatal exposure to the cyanobacterial toxin BMAA induces changes in protein expression and neurodegeneration in adult hippocampus. *Toxicol Sci* 2012;130:391-404.
  11. Lucarini E, Seguela L, Vincenzi M, Parisio C, Micheli L, Toti A, et al. Role of enteric glia as bridging element between gut inflammation and visceral pain consolidation during acute colitis in rats. *Biomedicines* 2021;9:1671.
  12. Manolakis AC, Kapsoritakis AN, Tiaka EK, Potamianos SP. Calprotectin, calgranulin C, and other members of the s100 protein family in inflammatory bowel disease. *Dig Dis Sci* 2011;56:1601-11.
  13. Duan K, Liu S, Yi Z, Liu H, Li J, Shi J, et al. S100-beta aggravates spinal cord injury via activation of M1 macrophage phenotype. *Musculoskelet Neuronal Interact* 2021;21:401-12.
  14. Yuan SM. S100 and S100beta: biomarkers of cerebral damage in cardiac surgery with or without the use of cardiopulmonary bypass. *Rev Bras Cir Cardiovasc* 2014;29:630-41.
  15. Yao Y, Liu F, Gu Z, Wang J, Xu L, Yu Y, et al. Emerging diagnostic markers and therapeutic targets in post-stroke hemorrhagic transformation and brain edema. *Front Mol Neurosci* 2023;16:1286351.
  16. Modi PK, Kanungo MS. Age-dependent expression of S100beta in the brain of mice. *Cell Mol Neurobiol* 2010;30:709-16.
  17. Hurley PA, Crook JM, Shepherd RK. Schwann cells revert to non-myelinating phenotypes in the deafened rat cochlea. *Eur J Neurosci* 2007;26:1813-21.
  18. Buckiová D, Syka J. Calbindin and S100 protein expression in the developing inner ear in mice. *J Comp Neurol* 2009;513:469-82.
  19. Pack AK, Slepecky NB. Cytoskeletal and calcium-binding proteins in the mammalian organ of Corti: cell type-specific proteins displaying longitudinal and radial gradients. *Hear Res* 1995;91:119-35.
  20. Osborn A, Caruana D, Furness DN, Evans MG. Electrical and immunohistochemical properties of cochlear fibrocytes in 3D cell culture and in the excised spiral ligament of mice. *J Assoc Res Otolaryngol* 2022;23:183-93.
  21. Yamashita H, Takahashi M, Bagger-Sjöbäck D. Expression of S-100 protein in the human fetal inner ear. *Eur Arch Otorhinolaryngol* 1995;252:312-5.
  22. Zimmer DB, Van Eldik LJ. Tissue distribution of rat S100 alpha and S100 beta and S100-binding proteins. *Am J Physiol* 1987;252:C285-9.
  23. Coppens AG, Kiss R, Heizmann CW, Schäfer BW, Poncelet L. Immunolocalization of the calcium binding S100A1, S100A5 and S100A6 proteins in the dog cochlea during postnatal development. *Brain Res Dev Brain Res* 2001;126:191-9.
  24. Liu WJ, Yang J. Developmental expression of inositol 1, 4, 5 trisphosphate receptor in the post-natal rat cochlea. *Eur J Histochem* 2015;59:2486.
  25. Liu WJ, Wang CX, Yu H, Liu SF, Yang J. Expression of acetylated tubulin in the postnatal developing mouse cochlea. *Eur J Histochem* 2018;62:2942.
  26. Hume CR, Bratt DL, Oesterle EC. Expression of LHX3 and SOX2 during mouse inner ear development. *Gene Expr Patterns* 2007;7:798-807.
  27. Szarama KB, Gavara N, Petralia RS, Chadwick RS, Kelley MW. Thyroid hormone increases fibroblast growth factor receptor expression and disrupts cell mechanics in the developing organ of Corti. *BMC Dev Biol* 2013;13:6.
  28. Liu WJ, Ming SS, Zhao XB, Zhu X, Gong YX. Developmental expression of high-mobility group box 1 (HMGB1) in the mouse cochlea. *Eur J Histochem* 2023;67:3704.
  29. Saegusa C, Kakegawa W, Miura E, Aimi T, Mogi S, Harada T, et al. Brain-specific angiogenesis inhibitor 3 is expressed in the cochlea and is necessary for hearing function in mice. *Int J Mol Sci* 2023;24:17092.
  30. Nakazawa K, Spicer SS, Gratton MA, Schulte BA. Localization of actin in basal cells of stria vascularis. *Hear Res* 1996;96:13-9.
  31. Matsunobu T, Schacht J. Nitric oxide/cyclic GMP pathway attenuates ATP-evoked intracellular calcium increase in supporting cells of the guinea pig cochlea. *J Comp Neurol* 2000;423:452-61.
  32. Berekméri E, Fekete Á, Köles L, Zelles T. Postnatal development of the subcellular structures and purinergic signaling of deiters' cells along the tonotopic axis of the cochlea. *Cells* 2019;8:1266.
  33. von Bohlen und Halbach O. Immunohistological markers for proliferative events, gliogenesis, and neurogenesis within the adult hippocampus. *Cell Tissue Res* 2011;345:1-19.
  34. Gattaz WF, Lara DR, Elkins H, Portela LV Gonçalves CA, Tort AB, et al. Decreased S100-beta protein in schizophrenia: preliminary evidence. *Schizophr Res* 2000;43:91-5.
  35. Oesterle EC, Sarthy PV, Rubel EW. Intermediate filaments in the inner ear of normal and experimentally damaged guinea pigs. *Hear Res* 1990;47:1-16.
  36. Moysan L, Fazekas F, Fekete A, Köles L, Zelles T, Berekméri E. Ca<sup>2+</sup> dynamics of gap junction coupled and uncoupled Deiters' cells in the organ of corti in hearing BALB/c mice. *Int J Mol Sci* 2023;24:11095.
  37. Rio C, Dikkes P, Liberman MC, Corfas G. Glial fibrillary acidic protein expression and promoter activity in the inner ear of developing and adult mice. *J Comp Neurol* 2002;442:156-62.
  38. Ladrech S, Wang J, Simonneau L, Puel JL, Lenoir M. Macrophage contribution to the response of the rat organ of Corti to amikacin. *J Neurosci Res* 2007;85:1970-9.
  39. Smeti I, Savary E, Capelle V, Hugnot JP, Uziel A, Zine A. Expression of candidate markers for stem/progenitor cells in the inner ears of developing and adult GFAP and nestin promoter-GFP transgenic mice. *Gene Expr Patterns* 2011;11:22-32.
  40. Hertzano R, Puligilla C, Chan SL, Timothy C, Depireux DA, Ahmed Z, et al. CD44 is a marker for the outer pillar cells in the early postnatal mouse inner ear. *J Assoc Res Otolaryngol* 2010;11:407-18.
  41. Bai X, Xu K, Xie L, Qiu Y, Chen S, Sun Y. The dual roles of triiodothyronine in regulating the morphology of hair cells and supporting cells during critical periods of mouse cochlear development. *Int J Mol Sci* 2023;24:4559.
  42. Yoshida A, Yamamoto N, Kinoshita M, Hiroi N, Hiramoto T, Kang G, et al. Localization of septin proteins in the mouse cochlea. *Hear Res* 2012;289:40-51.
  43. Johnen N, Francart ME, Thelen N, Cloes M, Thiry M. Evidence for a partial epithelial-mesenchymal transition in postnatal stages of rat auditory organ morphogenesis. *Histochem Cell Biol* 2012;138:477-88.
  44. Anttonen T, Belevich I, Kirjavainen A, Laos M, Brakebusch C, Jokitalo E, Pirvola U. How to bury the dead: elimination of apoptotic hair cells from the hearing organ of the mouse. *J Assoc*

- Res Otolaryngol 2014;15:975-92.
45. Whitlon DS. E-cadherin in the mature and developing organ of Corti of the mouse. *J Neurocytol* 1993;22:1030-8.
  46. Wangemann P. Supporting sensory transduction: cochlear fluid homeostasis and the endocochlear potential. *J Physiol* 2006;576:11-21.
  47. Ramírez-Camacho R, García-Berrocal JR, Trinidad A, González-García JA, Verdager JM, Ibáñez A, et al. Central role of supporting cells in cochlear homeostasis and pathology. *Med Hypotheses* 2006;67:550-5.
  48. Moyer JR Jr, Furtak SC, McGann JP, Brown TH. Aging-related changes in calcium-binding proteins in rat perirhinal cortex. *Neurobiol Aging* 2011;32:1693-706.
  49. Idrizbegovic E, Salman H, Niu X, Canlon B. Presbycusis and calcium-binding protein immunoreactivity in the cochlear nucleus of BALB/c mice. *Hear Res* 2006;216-217:198-206.
  50. Hu J, Ferreira A, Van Eldik LJ. S100beta induces neuronal cell death through nitric oxide release from astrocytes. *J Neurochem* 1997;69:2294-301.
  51. Esposito G, De Filippis D, Cirillo C, Sarnelli G, Cuomo R, Iuvone T. The astroglial-derived S100beta protein stimulates the expression of nitric oxide synthase in rodent macrophages through p38 MAP kinase activation. *Life Sci* 2006;78:2707-15.
  52. Ichihara S, Koshikawa T, Nakamura S, Yatabe Y, Kato K. Epithelial hyperplasia of usual type expresses both S100-alpha and S100-beta in a heterogeneous pattern but ductal carcinoma in situ can express only S100-alpha in a monotonous pattern. *Histopathology* 1997;30:533-41.
  53. Strepay D, Olszewski RT, Nixon S, Korrapati S, Adadey S, Griffith AJ, et al. Transgenic Tg(Kcnj10-ZsGreen) fluorescent reporter mice allow visualization of intermediate cells in the stria vascularis. *Sci Rep* 2024;14:3038.
  54. Qin T, So KKH, Hui CC, Sham MH. Pth1 is essential for cochlear marginal cell differentiation and stria vascularis formation. *Cell Rep* 2024;43:114083.
  55. Hibino H, Nin F, Tsuzuki C, Kurachi Y. How is the highly positive endocochlear potential formed? The specific architecture of the stria vascularis and the roles of the ion-transport apparatus. *Pflugers Arch* 2010;459:521-55.
  56. Quraishi IH, Raphael RM. Generation of the endocochlear potential: a biophysical model. *Biophys J* 2008;94:L64-6.
  57. Walters BJ, Zuo J. Postnatal development, maturation and aging in the mouse cochlea and their effects on hair cell regeneration. *Hear Res* 2013;297:68-83.
  58. Sadanaga M, Morimitsu T. Development of endocochlear potential and its negative component in mouse cochlea. *Hear Res* 1995;89:155-61.
  59. Lautermann J, ten Cate WJ, Altenhoff P, Grümmer R, Traub O, Frank H, et al. Expression of the gap-junction connexins 26 and 30 in the rat cochlea. *Cell Tissue Res* 1998;294:415-20.
  60. Zhong SX, Hu GH, Liu ZH. Expression of ENaC, SGK1 and Nedd4 isoforms in the cochlea of guinea pig. *Folia Histochem Cytobiol* 2014;52:144-8.
  61. Grygorowicz T, Welnia-Kamińska M, Strużyńska L. Early P2X7R-related astrogliosis in autoimmune encephalomyelitis. *Mol Cell Neurosci* 2016;74:1-9.
  62. Shirakawa H, Kaneko S. Physiological and pathophysiological roles of transient receptor potential channels in microglia-related CNS inflammatory diseases. *Biol Pharm Bull* 2018;41:1152-7.
  63. Vecino E, Rodriguez FD, Ruzafa N, Pereiro X, Sharma SC. Glia-neuron interactions in the mammalian retina. *Prog Retin Eye Res* 2016;51:1-40.
  64. Watson N, Ding B, Zhu X, Frisina RD. Chronic inflammation-inflammaging in the ageing cochlea: A novel target for future presbycusis therapy. *Ageing Res Rev* 2017;40:142-8.
  65. Verschuur C, Agyemang-Prempeh A, Newman TA. Inflammation is associated with a worsening of presbycusis: evidence from the MRC national study of hearing. *Int J Audiol* 2014;53:469-75.
  66. Raha-Chowdhury R, Raha AA, Henderson J, Ghaffari SD, Grigorova M, Beresford-Webb J, et al. Impaired iron homeostasis and haematopoiesis impacts inflammation in the ageing process in Down syndrome dementia. *J Clin Med* 2021;10:2909.
  67. Kaneko A, Naito K, Nakamura S, Miyahara K, Goto K, Obata H, et al. Influence of aging on the peripheral nerve repair process using an artificial nerve conduit. *Exp Ther Med* 2021;21:168.
  68. Son KH, Son M, Ahn H, Oh S, Yum Y, Choi CH, et al. Age-related accumulation of advanced glycation end-products-albumin, S100beta, and the expressions of advanced glycation end product receptor differ in visceral and subcutaneous fat. *Biochem Biophys Res Commun* 2016;477:271-6.
  69. Cruzana BC, Hondo E, Kitamura N, Matsuzaki S, Nakagawa M, Yamada J. Differential localization of immunoreactive alpha- and beta-subunits of S-100 protein in feline testis. *Anat Histol Embryol* 2000;29:83-6.
  70. Yang B, Liang G, Khojasteh S, Wu Z, Yang W, Joseph D, Wei H. Comparison of neurodegeneration and cognitive impairment in neonatal mice exposed to propofol or isoflurane. *PLoS One* 2014;9:e99171.
  71. Fujioka M, Okano H, Ogawa K. Inflammatory and immune responses in the cochlea: potential therapeutic targets for sensorineural hearing loss. *Front Pharmacol* 2014;5:287.

#### Online supplementary material

Figure S1. Double staining of S100β and phalloidin in the basal turn of E18.5 mouse cochlea.

Received: 24 January 2025. Accepted: 4 March 2025.

This work is licensed under a Creative Commons Attribution-NonCommercial 4.0 International License (CC BY-NC 4.0).

©Copyright: the Author(s), 2025

Licensee PAGEPress, Italy

European Journal of Histochemistry 2025; 69:4189

doi:10.4081/ejh.2025.4189

*Publisher's note: all claims expressed in this article are solely those of the authors and do not necessarily represent those of their affiliated organizations, or those of the publisher, the editors and the reviewers. Any product that may be evaluated in this article or claim that may be made by its manufacturer is not guaranteed or endorsed by the publisher.*